Formation of a non-diffractive Bessel-like beam from a metallic subwavelength aperture

Zhaofeng Li, K. B. Alici, H. Caglayan, and Ekmel Ozbay

Nanotechnology Research Center, Department of Physics, and Department of Electrical and
Electronics Engineering, Bilkent University, Bilkent, 06800 Ankara, Turkey
Email: zhaofengli@bilkent.edu.tr

Abstract

An electromagnetic non-diffractive Bessel-like beam from a subwavelength aperture is generated by placing a metallic circular grating-like structure in front of the aperture. When the incident wave is linearly polarized, the beam is axially asymmetric. The beam possesses fluctuating, but approximately uniform, intensity distribution along its longitudinal axis. The full width at half maximum of the beam remains less than two wavelengths over nearly ten wavelengths. Our experimental results are in good agreement with the simulation results.

1. Introduction

Since the discovery of Lezec and his co-workers [1,2], much effort has been devoted to the study of the beaming effect from a subwavelength aperture. There has been, so far, several theoretical and experimental works that investigated the underlying physics and optimization of the directivity for the beaming effect with the operation frequency, ranging from the optical to microwave regions. However, to the authors' best knowledge, there has been no demonstration of beaming formation from a subwavelength aperture for an important beam, i.e., a Bessel beam. The Bessel beam was first proposed by Durnin et al., who presented the concept of the non-diffractive propagation of an electromagnetic (EM) wave [3]. This concept makes it possible to reduce the inevitable diffractive spreading and is useful for many applications. The fundamental mode J_0 Bessel beam is essentially the interference pattern of a conical wave, which can be generated by means of axicons or diffractive elements. These methods either use a curved lens or calibrated beam as an incident wave. In the present report, we will demonstrate in the microwave region that a non-diffractive Bessel-like beam can be generated from a subwavelength aperture by adding a metallic circular grating-like structure in front of the aperture.

2. Results of simulation and experiments

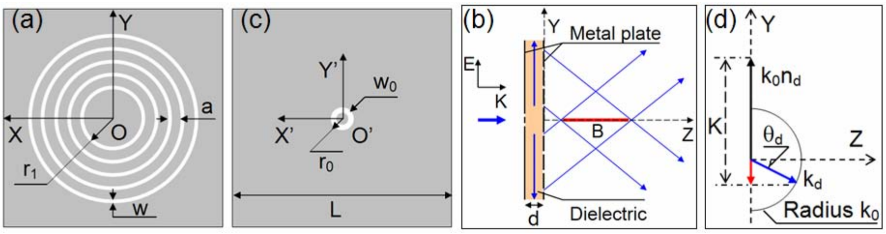

Fig. 1. (a) is the schematic of the front metal plate. (b) shows the back metal plate with an annular aperture. (c) shows the schematic for the formation of a Bessel-like beam (the B region). (d) shows the schematic for the calculation of θ_d.The black arrow (k_0n_d) is the radial wave vector. The blue arrow (k_d) is the wave vector of the diffracted wave.

Fig. 1 shows a schematic of the proposed structure. The structure comprises three parts, i.e., two metal plates (Copper with a thickness of 0.03 mm) sandwiching a dielectric layer. The side length L is 320 mm for the two square plates. The dielectric layer has a thickness d of 1.6 mm and refractive index n_d of 1.96. Fig. 1(a) shows the front part, which is a circular grating-like metal plate. For clarity, we schematically depict only five concentric rings. In fact, there are fifteen ring slits (with their radius r_1=20 mm, r_{15}=146 mm, and a period of the rings a=9 mm), in which the width w of these slits is 1

ISBN 978-0-9551179-6-1

mm. Fig. 1(b) is the back part, which is a metal plate with a subwavelength annular aperture for the incident wave. The radius r_0 and width w_0 of the annular aperture are 5 mm and 2 mm, respectively. Fig. 1(c) shows the schematic process for the formation of a non-diffractive beam. Fig. 1(d) shows the dependence of the diffraction angle θ_d on the wave number of the grating ($\mathsf{K}=2\pi/a$) and the wave vector of the radially propagating wave ($k_0 n_d$). It is easy to obtain the following relation,

$$\sin\theta_d = (k_0 n_d - \mathsf{K})/k_0 \tag{1}$$

We choose the wavelength of the EM wave in the dielectric media to be larger than the periodic constant of the rings, so that ($k_0 n_d$-K) and θ_d are both negative, which means that the diffracted waves all travel towards the central *z* axis. Consequently, the interference of these waves in turn forms a non-diffractive Bessel-like beam. Furthermore, the length of the line focus L_f of the Bessel-like beam can be estimated according to geometric optics as

$$L_f \approx 14a/\tan\theta_d \tag{2}$$

In the present study, three-dimensional finite-difference time-domain simulation was carried out. An EM wave with its *E* field polarized in the *y* direction is incident on the subwavelength aperture. The emitted wave beam will have its *E* field mainly in the *y* direction and, therefore, we present here the E_y field results of our simulation for a convenient comparison with our experimental results.

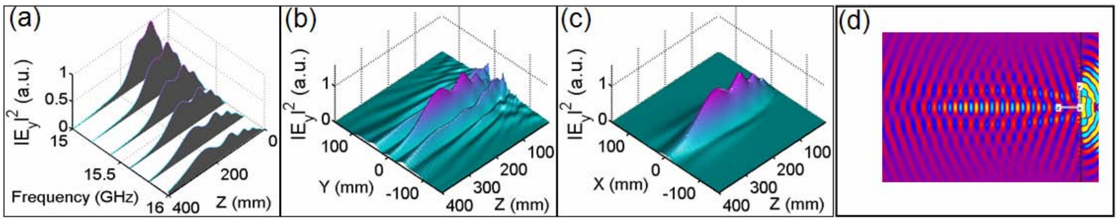

Fig. 2. Simulation results. (a) shows the intensity distribution of E_y along the *z* axis at six different frequencies. (b) and (c) show the intensity distribution of E_y on the *xz* and *yz* plane, respectively. (d) is a snapshot of E_y for the wave propagation on the *yz* plane.

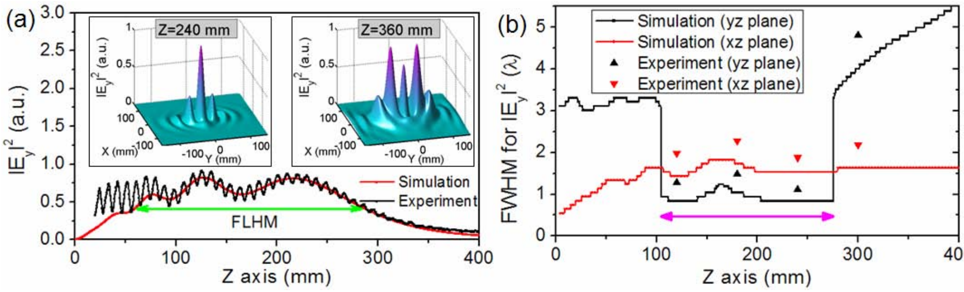

Fig. 3. (a) shows the simulation and experimental results for the intensity distribution of E_y along the *z* axis. The two insets show the simulation results for the intensity distributions of E_y at two different cross sections. (b) shows the FWHM data for the Bessel-like beam.

Fig. 2(a) shows the simulation results for the E_y intensity distributions along the *z* axis at frequencies ranging from 15 to 16 GHz with an interval of 0.2 GHz. It is clearly seen that along with the increase of the operation frequency, the effective length of the beam also increases. These results are consistent with our estimations according to Eq. (1) and (2). Due to space constraints, in the following part we will only concentrate on one typical beam of frequency f=15.8 GHz (λ=18.99 mm) in order to investigate its detailed features. Fig. 2(b) and (c) are the E_y intensity distributions on the *xz* and *yz* planes, respectively. One can clearly see that a beam is formed along the *z* axis, and the beam is axially asymmetric. Fig. 2(d) shows a snapshot of the wave propagation on the *yz* plane, from which it can be seen that two symmetric diffracted waves are emitted from the front metal plate with a regular wave front. These waves travel towards to the *z* axis, where their interference forms the non-diffractive Bessel-like beam just as we expected. We plot the E_y intensity distribution along the *z* axis in Fig. 3(a) as a solid red curve. The full length at half maximum (FLHM) of the Bessel-like beam is approx. 226 mm, as indicated by a green line with double arrows in the figure. In Fig. 3(a) one also sees that the intensity fluctuates along the *z* axis, and after the beam reaches a critical length (at approx. $z = 280$ mm), the intensity decreases rapidly to a very low level. The insets of Fig. 3(a) illustrate two typical E_y intensity distributions for the cross sections at $z = 240$ mm and 360 mm. It is rather clear that within the critical length, there is a high intensity main lobe at the center. However, when the *z* distance exceeds the critical length, the central lobe becomes weaker and the side lobes become much stronger, which means that the energy no longer remains in a small central area. Besides, we measured the full width at half maximum (FWHM) for the beam. The solid lines in Fig. 3(b) show the results of the simulation. The abrupt jumping of the FWHM data for the *yz* plane is due to the evolution of side lobes. Considering the data on the *yz* and *xz* planes, it can be seen that there is a range of approx. 9 wavelengths within which both FWHMs remain less than 2 wavelengths.

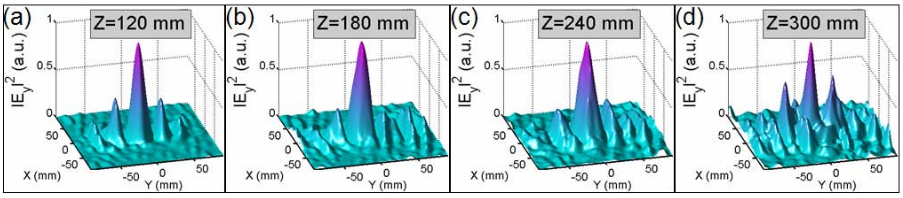

Fig. 4. (a), (b), (c), and (d) are the experimental results for the intensity distributions of E_y at four different cross sections.

To verify the above simulation results, we conducted experiments for the structure of Fig. 1. An HP-8510C network analyzer was used to excite a horn antenna in order to obtain a *y* polarized incident EM field. A standard Ku band waveguide antenna was used to receive and measure the EM wave that was emitted from the front metal plate. We plot the measured E_y intensity distribution along the *z* axis in Fig. 3(a) as a solid black curve, on which one sees a dense tapered oscillation. The oscillation becomes weaker at farther *z* positions. The period of the oscillation (approx. 9.5 mm) is approx. half of one wavelength and, therefore, this tapered oscillation should come from the Fabry-Perot effect between the front metal plate and the receiver antenna. Besides, we scanned the E_y intensity distributions on the cross sections at four *z* axis distances (z=120, 180, 240, and 300 mm), from which the FWHMs of the beam are also measured. The FWHM results are plotted as discrete triangles in Fig. 3(b). Fig. 4 shows the four recorded E_y intensity distributions on the cross sections at the four *z* axis distances. The intensity distributions that are shown in Fig. 4(a), (b), and (c) are at the z axis positions within the critical range, in which they all have high intensity main lobes at the center. However, the intensity distribution of Fig. 4(d) is at the z axis position farther than the critical length, and consequently the side lobes grow rapidly and lead to a large FWHM, as shown in Fig. 3(b). Conclusively, the experimental results confirmed our simulation results.

3. Conclusion

We demonstrate via simulation and experiment that a non-diffractive Bessel-like beam can be generated from a metallic subwavelength aperture by placing a metallic grating-like structure in front of the aperture. When the incident wave is linearly polarized, the beam shows axial asymmetry. Although the present study is at the microwave frequency, the principle can be extended to the optical region straightforwardly.

References

[1] H. J. Lezec, A. Degiron, E. Devaux, R. A. Linke,L. Martin-Moreno, F. J. Garcia-Vidal, and T. W. Ebbesen, Beaming Light from a Subwavelength Aperture, Science, vol. 297, no. 5582, pp. 820-822, 2002.

[2] T. Thio, K. M. Pellerin, R. A. Linke,H. J. Lezec and T. W. Ebbesen, Enhanced light transmission through a single subwavelength aperture, Opt. Lett., vol. **26**, no. 24, pp. 1972-1974, 2001.

[3] J. Durnin and J. J. Miceli, Jr., Diffraction-free beams, Phys. Rev. Lett., vol. 58, no. 15, pp. 1499-1501, 1987.